

Properties of Polyamic Acid Ionomers

XUEHAI YU,¹ BRIAN P. GRADY,² RICHARD S. REINER,² and S. L. COOPER^{2,*}

¹Department of Chemistry, Nanjing University, People's Republic of China; and ²Department of Chemical Engineering, University of Wisconsin, Madison, Wisconsin 53706

SYNOPSIS

Polymers containing amic acid units were produced by reacting an oligomer based on polytetramethylene oxide (PTMO) with 1,2,4,5-benzenetetracarboxylic dianhydride (BTDA). Neutralization by a metal salt produced amic acid ionomers. Similar to other ionomer systems, neutralization from the acid to the ionomer led to the formation of a separate ionic phase as determined by dynamic mechanical analysis. Phase separation resulted in a substantial increase in mechanical properties. The effect of neutralization level, cation, soft-segment molecular weight, and soft-segment end group on mechanical and thermal properties was investigated. © 1993 John Wiley & Sons, Inc.

I. INTRODUCTION

Ionomers contain a small mole fraction (usually less than 10 mol %) of ionic groups chemically bonded to the polymer chain. Introduction of ionic moieties causes improved properties including increased toughness, tear strength, and abrasion resistance.¹ Many different polymer backbones have been modified by introduction of ionic groups including polyethylene, polystyrene, and polytetrafluoroethylene.

Polyurethanes are formed by reacting an oligomer diol (typical molecular weight 1000–5000) with a diisocyanate. The diisocyanate usually contains at least one aromatic ring. A short-chain diol can be added to the mixture as well. The short-chain diol connects diisocyanates, which concentrate aromatic rings along the polyurethane chain. Incompatibility between the aromatic ring and the oligomer can cause microphase separation without ionization. Because the glass transition of the oligomer is below room temperature, the oligomer is designated the soft segment. The glass transition of the phase containing aromatic rings is usually above room temperature, so the diisocyanate-chain extender adduct is termed the hard segment. The short-chain diol, if present, is called the chain extender, because this

molecule, when used in prepolymer formation, extends the hard segment molecular weight.

Ionic groups can be grafted on the urethane nitrogens to produce ionomers. The properties of such polyurethane ionomers synthesized from a 1 : 1 stoichiometric ratio of isocyanate and polyol (not chain-extended) have been extensively studied in our laboratory. Because the hard segment has not been chain-extended, these materials do not microphase separate without ionization. The mechanical properties,^{2–4} small-angle X-ray scattering characteristics,^{5,6} and local cation environment^{7,8} have been studied in sulfonated polyurethanes based on toluene diisocyanate (TDI) hard segments. Carboxylated polyurethanes with TDI hard segments have been produced by grafting an ethylcarboxylate linkage solely at the urethane hydrogen.² Sulfonated polyurethanes with a methylene bis(*p*-phenyl isocyanate) (MDI) hard segment have also been analyzed.^{9,10}

The effect of hard-segment length in sodium-neutralized sulfonated polyurethane ionomers was investigated in a polytetramethylene oxide (PTMO)-MDI system chain-extended with butanediol (BD).¹¹ The mole ratios MDI-BD-PTMO investigated were 3 : 2 : 1 and 1 : 0 : 1. The polyurethane without chain extender was not phase-separated prior to ionization, and introduction of ionic groups increased soft-segment phase purity, improved mechanical properties dramatically, and extended the storage modulus to much higher temperatures before reaching

* To whom correspondence should be addressed.

the terminal zone. In the chain-extended material, which was phase-separated prior to ionization, low levels of ionization initially disrupted soft-segment phase purity without significantly affecting mechanical properties. At higher sulfonation levels, the soft-segment phase purity was again high and the mechanical properties were substantially higher as well.

Another method of producing polyurethane ionomers is to include the ionic functionality in the chain extender. Carboxylated polyurethane ionomers were synthesized from an MDI hard-segment chain extended with bis(hydroxymethyl)propanoic acid and a PTMO soft segment.¹² Neutralization of acid groups in the poorly phase-separated carboxylated polyurethane caused a large increase in the phase separation. The cations Li^+ , Na^+ , and K^+ were similar in their effect on the mechanical properties.

The effect of PTMO molecular weight was studied in sulfonate polyurethane ionomers based on MDI chain-extended with methyl diethanolamine (MDEA).¹³ The mol ratio MDI-MDEA-PTMO was 3 : 2 : 1. The MDEA was reacted with γ -propyl sulfone and the resulting zwitterionomer was reacted with a metal acetate to produce the ionomer. The plateau modulus for the unionized material based on PTMO-2000 extended to much higher temperatures than did the unionized polyurethane based on PTMO-1000. Ionization of this material resulted in little change in the physical properties. In contrast, ionization of the polyurethane based on PTMO-1000 resulted in a marked improvement in physical properties.

Aromatic polyimides are used in a wide variety of specialty applications because of their excellent thermal and mechanical properties. Commercially available polyimides include Kapton® (DuPont) and ULTEM® (G.E.). Extremely high thermoforming temperatures and insolubility in most solvents makes processing of polyimides very difficult. Recent papers¹⁴⁻¹⁶ and a patent application¹⁷ describe the synthesis of polyimides with flexible sequences in the polymer backbone. These efforts have led to materials that are soluble in some common solvents as well as being processible at lower temperatures.

In a previous study,¹⁸ segmented polyimides were synthesized from poly(tetramethylene oxide) glycol di-*p*-aminobenzoate (marketed under the trade name Polamine®) and benzenetetracarboxylic dianhydride (BTDA). The fully imidized form had the properties of a tough thermoplastic elastomer. Neutralizing the amic acid prior to imidization with a stoichiometric amount of sodium also produced a

material with the properties of a tough thermoplastic elastomer. This study explores amic acid ionomers in more detail.

II. EXPERIMENTAL

Materials and Synthesis

Three different oligomers were used. Polamine (POL) was obtained from the Air Products Corporation. Polytetramethylene (PTMO) diol was purchased from Quaker Oats. The oligomers were dried under vacuum at 70°C for 24 h and stored in a desiccator immediately prior to use. BTDA (97% anhydride with the remainder free acid) was purchased from the Aldrich Chemical Co. and recrystallized in acetic anhydride before use.

The material containing Polamine was synthesized under a dry argon atmosphere at room temperature in THF. BTDA, 15 wt %, in THF was added to a THF solution containing a stoichiometric amount of Polamine. The exothermic reaction caused the temperature to rise to approximately 40°C briefly. The solution was stirred overnight to guarantee reaction completion. The amic acid polymer was precipitated in methanol, filtered, and dried for 24 h at 70°C under vacuum. A schematic of the synthesis is shown in Figure 1.

The material containing hydroxy-terminated PTMO was synthesized in toluene. A stoichiometric amount of BTDA was added to the oligomer solution and the suspension was refluxed for 4 h, when the solution became clear. The toluene was removed by distillation and the product was dried.

The acid precursor was redissolved in THF. A calculated amount of the appropriate metal acetate was added. Ionomers synthesized from Polamine did not precipitate so the samples were cast directly onto Teflon dishes from the THF solution. The other PTMO-based ionomer precipitated from the THF solution. This polymer was removed from the THF solution and dried, then dissolved in a 50/50 mix of acetic acid/DMAc and cast onto a Teflon dish. The Teflon dish containing the samples was placed in a 65°C convection oven until the material was partially dry, then transferred to a vacuum oven at 70°C for 24 h. This procedure resulted in films approximately 0.1 mm thick. Film thickness varied significantly from sample to sample.

Sample Designation

The system employed to designate the samples is illustrated by the example "POL-650-Cu-100." The

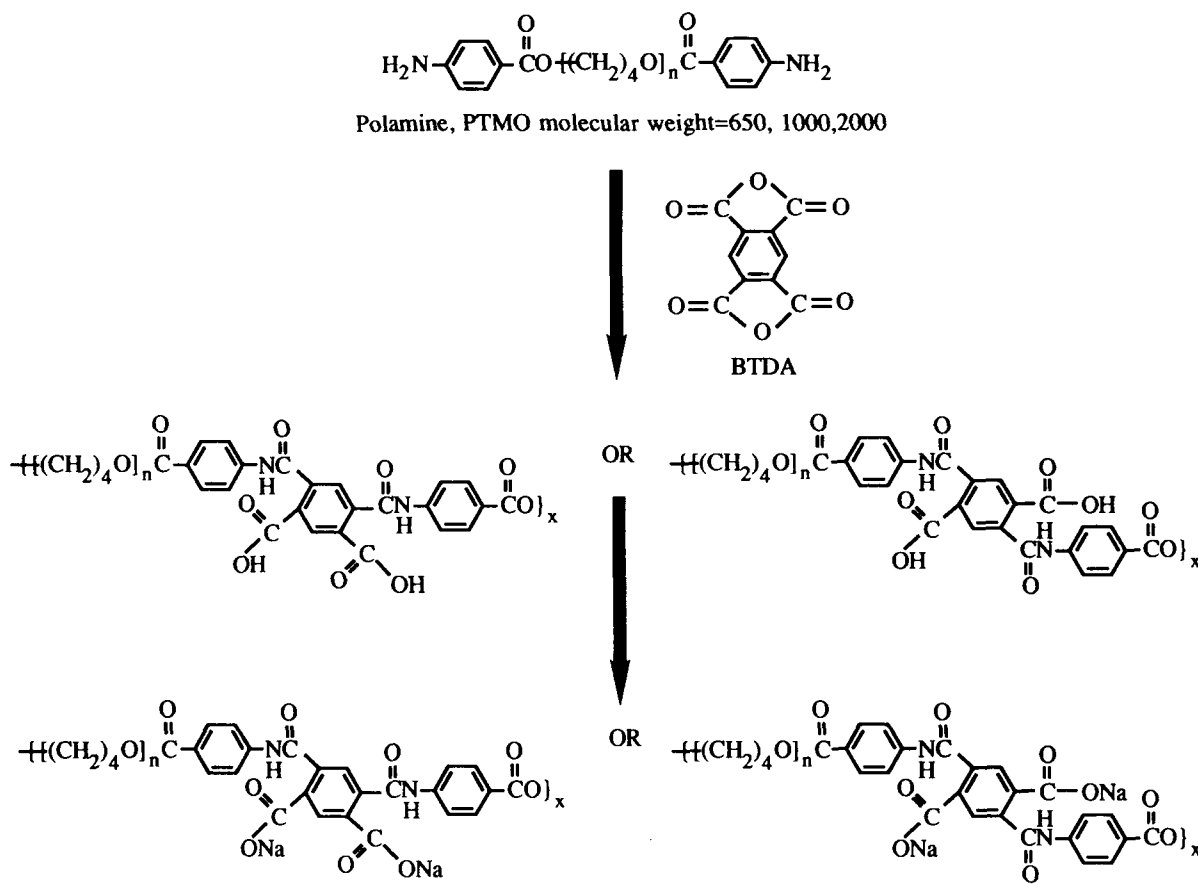


Figure 1 Synthesis of amic acid ionomers.

first letters indicate the soft segment (POL or PTMO) followed by the soft-segment molecular weight (not including terminating groups), neutralizing cation, and, finally, neutralization percentage. One hundred percent neutralization means that all acid groups were neutralized with the metal cation.

Characterization Methods

1. Stress-Strain

Uniaxial stress-strain measurements were made with a table model Instron at room temperature using a crosshead speed of 0.5 in/min. Samples were cut from cured films using an ASTM D1708 die. All measurements represent the average of three runs. Engineering stress was calculated based on the initial area of the sample. Table I lists the tensile properties for the materials examined in this study.

2. Differential Scanning Calorimetry (DSC)

DSC measurements were made on a Perkin-Elmer DSC 2 equipped with a 3500 series data station or

a Perkin-Elmer DSC 7 with a 7500 series data station. Temperature calibration was via mercury and indium standards. Indium was used to calibrate enthalpy measurements. The measurements were performed under a helium purge at a heating rate of 20°C. The only feature in the DSC spectra for all

Table I Tensile Properties of Amic Acid Ionomers

Material	Modulus (MPa)	Ultimate Elongation	Ultimate Stress (MPa)
POL-650-Acid	12.6	88	4.8
POL-650-Cu-25	62.6	179	18.5
POL-650-Cu-50	143	171	33.1
POL-650-Cu-100	359	102	32.8
POL-650-Na-100	108	52	11.7
POL-650-Ni-100	106	68	18.6
POL-650-Zn-100	14.1	45	2.5
POL-1000-Cu-100	93.1	435	62.1
PTMO-1000-Cu-100	86.9	500	34.4
POL-1900-Cu-100	34.5	325	11.4

samples in this study was a soft-segment-rich phase glass transition. The hard-segment or ionic phase did not exhibit a transition in the DSC curves, which is similar to observations in polyurethane ionomers.^{2,3}

Glass transition temperatures were determined via the following method: Lines were drawn along the approximately linear DSC trace above and below the glass transition. A third line was drawn corresponding to the slope at the inflection point of the glass transition. The glass transition temperature was calculated as the average of intersection points between the third line and the two other lines. The heat-capacity change was calculated at T_g from the vertical distance between the two extrapolated DSC traces.

3. Dynamic Mechanical Thermal Analysis (DMTA)

A Rheometrics RSA II in the tension mode was used to acquire DMTA spectra. Samples were cut using an ASTM D1043 die with the ends cut to the proper length. The approximate test dimensions were $23 \times 6.3 \times 1$ mm. The autotension mode was used with a 120% force for pretension. Three-degree temperature steps with a 0.1 min soak time were used. It was found that increasing the soak time to 1 min did not affect the spectra. The test frequency was 16 Hz over the temperature range from -150 to 300°C . In the DMTA spectra displayed in this paper, the loss modulus has been reduced by a factor of 10 for clarity of presentation.

III. RESULTS

Effect of Neutralization

Neutralization with copper affected the tensile properties of the acid substantially, as shown in Figure 2 for materials based on the soft segment POL-650. The modulus and stress at break increased as the neutralization level increased. The stress at break reached a plateau value at 50% neutralization. The ultimate strain increased initially upon neutralization, then decreased between samples at 50% neutralization and 100% neutralization.

The properties of the acid were not reproducible for three different samples. In DMTA experiments, the rubbery plateau extended out to different temperatures before the terminal zone was reached. Presumably, the amic acid was undergoing partial imidization during storage at room temperature. Storage time was not controlled for the materials in this study. The properties of the acid reported in

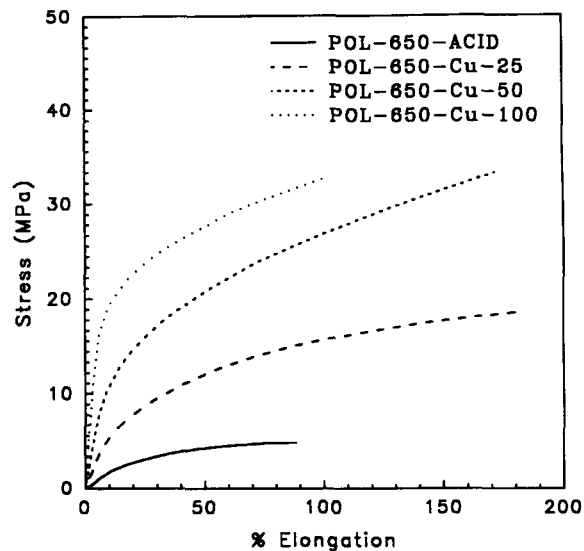


Figure 2 Effect of neutralization on the stress-strain curve for POL-650-Cu-x.

this paper are for the material where the terminal zone occurred at the lowest temperature. The results for the fully neutralized material were reproducible from sample to sample, indicating imidization of the ionomers did not occur at room temperature over the time frame of weeks. No reproducibility studies were made for the partially neutralized samples.

E' and E'' curves of copper-neutralized POL-650 are shown in Figure 3. The transition in E'' , which appeared at 250°C upon neutralization, indicates that a separate ion-rich phase emerged in the material. This transition has recently been attributed to an ionic-phase glass transition.¹⁹ Only materials with 50% and 100% neutralization had a clearly defined ion-rich phase transition. At temperatures below the ionic transition, the ionic domains act as cross-links in the material. The increase in modulus indicated a greater number of sites were available for cross-linking in the 100% neutralized material vs. the 50% neutralized material.

The phantom network theory models a polymer network as chains interconnected at cross-link points. The flat storage modulus between 0 and 200°C suggests that this model can be applied as a first approximation with the aggregates acting as cross-link points. The phantom network theory^{20,21} predicts Young's modulus E will be given by

$$E = 3 \left(\frac{f-2}{f} \right) \nu RT \quad (1)$$

where f is the cross-link functionality; ν , the cross-link density; R , the gas constant, and T , the tem-

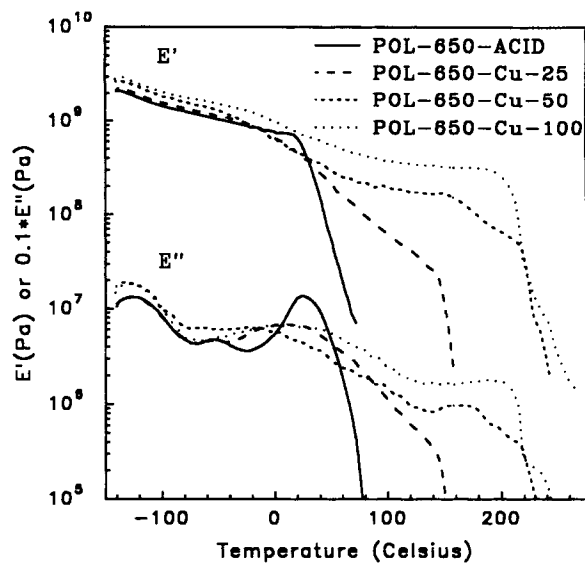


Figure 3 Effect of neutralization on E' and E'' for Pol-650-Cu- x . E'' has been multiplied by 0.1 for clarity.

perature. Based on this model, an increase in modulus upon neutralization could be due to an increase in cross-link density and/or an increase in cross-link functionality. An increase in neutralization level from 50 to 100% caused the modulus to jump by a factor of 2.5. Since the maximum increase in modulus due to functionality differences is a factor of 2, the modulus rise was due to either a combination of functionality and cross-link density changes or just a change in the cross-link density alone.

The effect of neutralization level was studied in sulfonated polystyrene.²² Changing the neutralization level from 50 to 100% did not change the position of the ionomer SAXS peak. If the scattering peak is due to interparticle interference and the location of the peak maximum is a rough measure of interparticle distance,²³ then an increase in neutralization level did not result in an increase in aggregate density. However, a similar type of neutralization study on a carboxylated polyurethane showed that the peak position shifted to lower angles as the neutralization level increased, which indicated a decrease in aggregate density as the neutralization level increased.⁵ These results suggest that ionic aggregates are not the only effective cross-links in ionomers.

In a study comparing carboxylated and sulfonated anions in the same base polyurethane,^{2,5} the tensile moduli were equivalent even though the Bragg spacing corresponding to the SAXS peak was much larger in the carboxylate ionomer. The authors attributed the equivalence of moduli to a larger number

of entanglements in the carboxylate ionomer. The authors concluded that ionic aggregation increased the number of entanglements, which acted as effective cross-links in the material.

In the amic acid materials, if the relative degree of phase separation is the same in both the 50 and 100% neutralized material and only ionic aggregates act as effective cross-links, then the maximum increase in modulus based on the phantom network model would only be a factor of 2. However, more chains would be tied to aggregates in the 100% neutralized material, which should increase the number of entanglements. If these entanglements act as effective cross-links, then the rise in modulus would be greater than a factor of 2.

The filler effect, rather than entanglements, could also explain the increase in modulus above that predicted by simple aggregate density effects. A simple calculation using the Guth–Smallwood equation²⁴ shows that the cation + anion alone cannot solely account for the extent of the modulus increase. If one postulates an immobilization effect of the polymer matrix as suggested by Eisenberg et al.,²⁵ then this mechanism could explain the rise in the modulus.

DSC curves for the neutralized samples were featureless. The highly phase-mixed acid material exhibited a PTMO-rich-phase glass transition at a temperature much higher than that of pure PTMO. The lack of a noticeable glass transition in the neutralized samples was probably caused by a small weight fraction of the relatively pure PTMO phase in conjunction with extremely short PTMO chains. To create a phased-mixed material that would show a noticeable transition, after reaching 175°C, the material was quickly quenched and the DSC experiment repeated. The results shown in Table II are from the second run for all materials except the acid and demonstrate that the driving force for a pure PTMO phase increases as the ionization level increases.

Table II Effect of Neutralization Level on Soft-segment Glass Transition^a

Material	T_g (°C)	ΔC_p (cal/g K)
POL-650-ACID	-24	0.338
POL-650-Cu-25	-34	0.115
POL-650-Cu-50	-39	0.116
POL-650-Cu-100	-47	0.133

^a All data in this table except for the acid are taken from the second DSC run; see text for explanation.

Effect of Counterion

Materials with the soft-segment POL-650 were used to study the effect of neutralizing cation type on properties. Four different cations were studied: Cu^+ , Na^+ , Ni^{2+} , and Zn^{2+} . The zinc-neutralized material behaved very similarly to the pure acid. Ding et al.² showed that zinc-neutralized sulfonated polyurethane ionomers were substantially weaker than were sodium or nickel based materials. The authors concluded that the zinc-neutralized material had the largest number of ionic groups dissolved in the matrix. In the amic acid ionomers studied here, DMTA spectra of the zinc ionomer shows no high-temperature transition corresponding to an ion-rich phase in this system. Apparently, the energetics do not favor phase separation in the zinc-neutralized ionomer. The three other counterions induced phase separation as seen in Figure 4. The nickel-neutralized material never developed a peak in E'' corresponding to the ionomer transition. This sample broke at approximately 275°C. The upturn in E'' immediately before the sample failed may have been due to the onset of an ionic transition.

Stress-strain curves are shown in Figure 5. The tensile modulus decreased in the order $\text{Cu}^{2+} > \text{Ni}^{2+} = \text{Na}^+ > \text{Zn}^{2+}$. The tensile modulus was approximately a factor of 3 greater for the Cu^{2+} ionomer than for Ni^{2+} or Na^+ . Clearly, the degree of phase separation was highest for the copper-based material. The ultimate elongation was also greater for

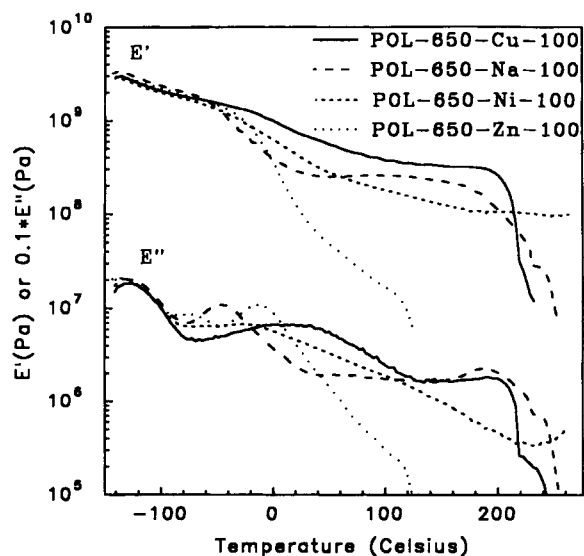


Figure 4 Effect of cation on E' and E'' for POL-650-x-100. E'' has been multiplied by 0.1 for clarity.

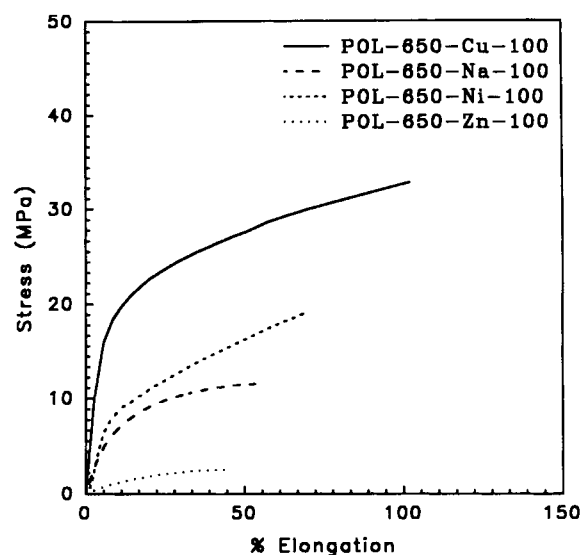


Figure 5 Effect of cation on the stress-strain curve for POL-650-x-100.

the copper-neutralized material. Whereas the copper-neutralized material was mechanically superior at room temperature, the nickel-based material had ionic aggregates that were thermally more stable.

The copper- and nickel-based materials did not have discernible soft-segment glass transitions in DSC scans. Because the soft-segment phase was not contaminated with as much hard segment as the other materials, not enough material existed in the soft-segment phase to cause a large enough change in the heat capacity to be observed by DSC. The glass transition temperature for zinc and the acid materials were very similar, as shown in Table III, consistent with the conclusion zinc did not induce phase separation. The glass transition was approximately 20°C lower for the sodium-neutralized material, indicating that the soft-segment phase was much purer in the sodium-neutralized material.

Table III Effect of Cation on Soft-segment Glass Transition

Material	T_g (°C)	ΔC_p (cal/g K)
POL-650-Cu-100	^a	^a
POL-650-Na-100	-53	0.148
POL-650-Ni-100	^a	^a
POL-650-Zn-100	-31	0.133
POL-650-ACID	-24	0.338

^a The change in heat capacity for this material was insufficient to measure a glass transition temperature.

Effect of Soft Segment

1. Soft-segment Molecular Weight

As the soft-segment molecular weight increased, the distance between ionic groups increased and the hard-segment fraction decreased. Stress-strain curves in Figure 6 for materials neutralized with copper demonstrate that the modulus and stress at break were lowered as the soft-segment molecular weight increased, agreeing with the expected behavior. Since the cross-link density is inversely proportional to the molecular weight between cross-links, one might expect the modulus to decrease by a factor of 1.5 between POL-650 and POL-1000 and by a factor of 3 between POL-650 and POL-1900. The actual factors in this study were 4 and 10, respectively, which indicated that the number of aggregates was greater in the lower molecular weight material and/or aggregates were not the only effective cross-links in the material.

In polyurethane ionomers, an inverse linear relationship between soft-segment molecular weight and Young's modulus has been seen in two studies. In TDI-based sulfonated polyurethane ionomers with PPO and PTMO soft segments, such an effect was seen when the molecular weight was varied between 1000 and 3000.² For MDI-PTMO sulfonated polyurethanes, the PTMO soft-segment molecular weight was inversely proportional to the modulus.¹⁰ In a different study involving sulfonated polyurethanes based on TDI/PTMO,³ the modulus decreased more rapidly than an inverse linear relationship would predict, similar to the results in this

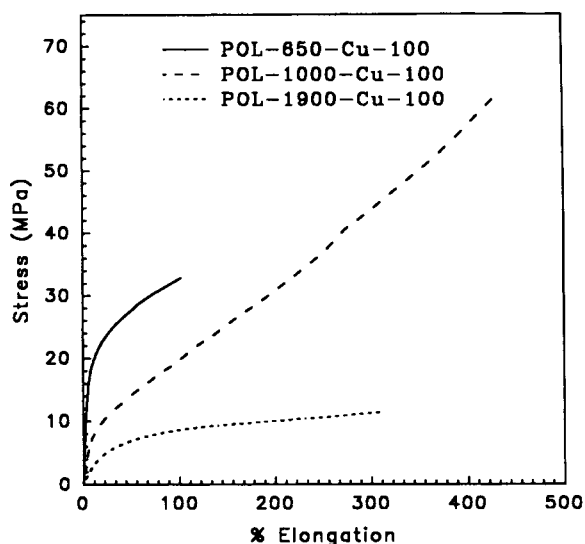


Figure 6 Effect of soft-segment molecular weight on the stress-strain curve for POL-x-Cu-100.

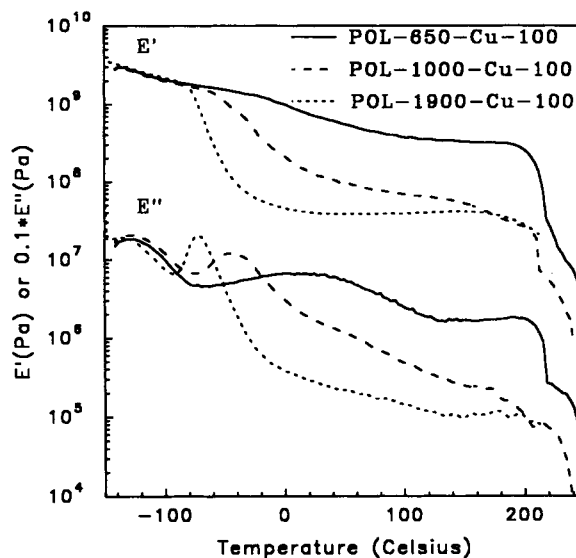


Figure 7 Effect of soft-segment molecular weight on E' and E'' for POL-x-Cu-100. E'' has been multiplied by 0.1 for clarity.

study. Finally, in chain-extended polyurethanes with PTMO-MDI-MDEA,¹³ the modulus decreased faster than an inverse linear relationship would predict. Clearly, the relationship between modulus and soft-segment molecular weight is not simple.

DMTA curves of copper-neutralized ionomers of varying soft-segment molecular weight are shown in Figures 7 and 8. The rubbery plateau modulus drops as the soft-segment molecular weight increases, consistent with stress-strain results. The temperature of the ionic transition was independent of soft-

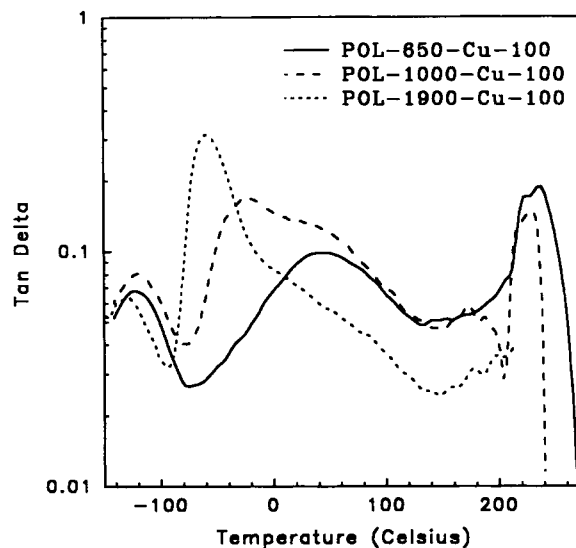


Figure 8 Effect of soft-segment molecular weight on $\tan \delta$ for POL-x-Cu-100.

Table IV Effect of Soft-Segment Properties on Soft-segment Glass Transition

Material	T_g ($^{\circ}\text{C}$)	ΔC_p (cal/g K)
POL-650-Cu-100	^a	^a
POL-1000-Cu-100	-55	0.245
POL-1900-Cu-100	-73	0.314
PTMO-1000-Cu-100	-64	0.346

^a The change in heat capacity for this material was insufficient to measure a glass transition temperature.

segment molecular weight. One would not expect the soft-segment characteristics to influence the temperature of the ionic transition. The amount of material involved in the ionic transition (proportional to the area under the $\tan \delta$ vs. temperature curve) increases as the soft-segment molecular weight decreases.

The soft-segment glass transition temperature dropped from -55 to -73°C as the soft segment molecular weight increased from 1000 to 1900 (Table IV). As was discussed previously, the heat-capacity difference for the soft-segment phase in POL-650-Cu-100 was insufficient to appear as a noticeable glass transition in DSC experiments. Two factors could explain the inverse relationship between soft-segment molecular weight and soft-segment glass transition temperature. Soft-segment atoms close to the aromatic rings would be relatively immobile during the soft-segment glass transition because the

temperature is far below the hard-segment glass transition temperature. A higher temperature would be needed to induce the long-range cooperative motion in the soft-segment characteristic of the glass transition. Since the percentage of endgroups is higher for the lower molecular weight material, the glass transition temperature should be higher for the lower molecular weight material. Such an explanation has been advanced for sulfonated polyurethanes² and un-ionized segmented polyurethanes.²⁶ The other possible factor could be that the higher molecular weight led to an improvement in soft-segment phase purity, which would also cause the glass transition temperature to drop. No soft-segment crystallization endotherms were apparent in the DSC curves.

2. Effect of Endgroup

Ionomers with PTMO-1000 diol soft segments were synthesized. The hard segment consisted of three aromatic rings in POL-1000 and only one aromatic ring in PTMO-1000, as shown in Figure 9. The linkage between hard and soft segment was an amide for the POL material and an ester for the PTMO material. The molecular weight of 1000 refers to the molecular weight of PTMO repeat units only, i.e., $n = 14$ in Figure 9 for both POL-1000 and PTMO-1000.

Young's modulus is equivalent for the two materials, as shown in Figure 10. The stress at break is higher for the POL material, because the hard-

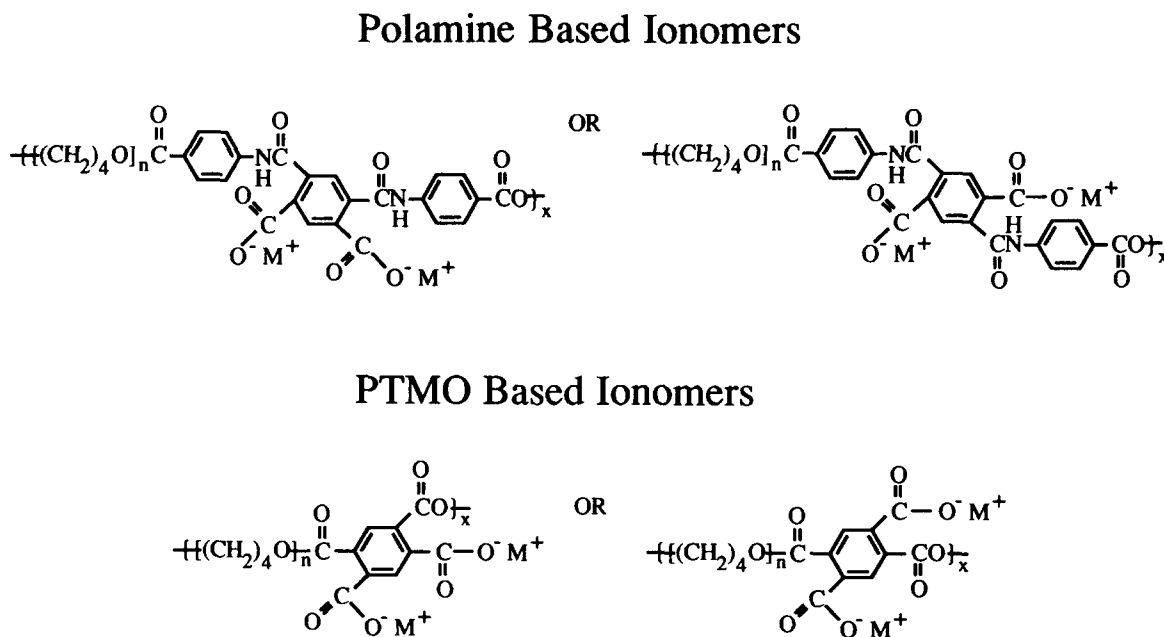


Figure 9 Structure of Polamine and PTMO diol-based ionomers.

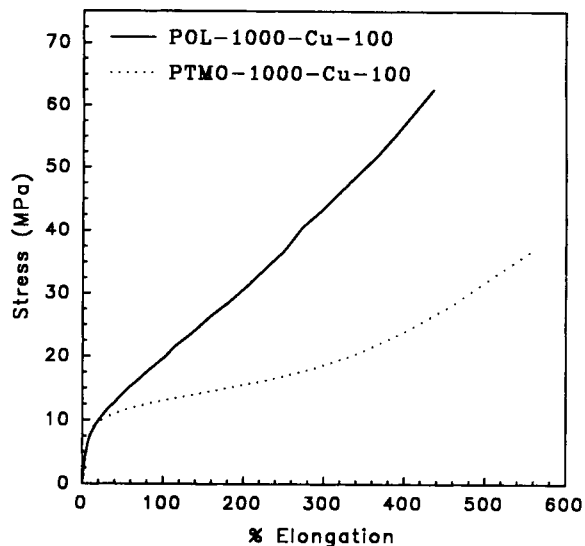


Figure 10 Effect of hard-segment length on stress-strain curve.

segment weight fraction in this material is significantly higher. The rubbery plateau modulus is extremely flat for the PTMO material compared to the POL material, as shown in Figure 11. The number of aromatic rings in the hard segment did not affect the ionic transition temperature as shown in Figure 12.

The soft-segment glass transition temperature was substantially lower in the PTMO diol-based ionomer. This was not a molecular weight effect since the PTMO molecular weight in both materials

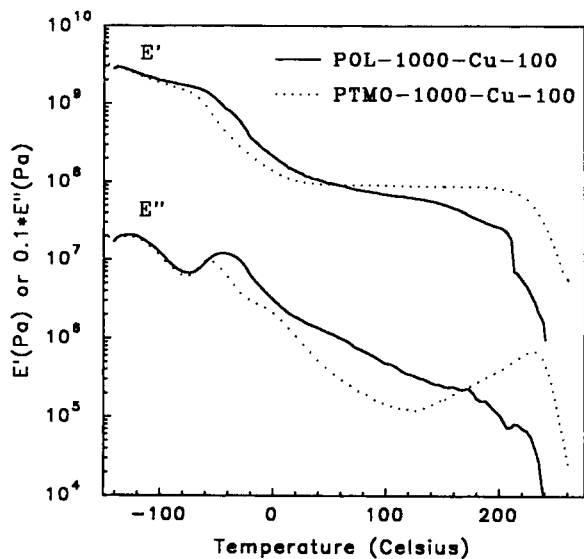


Figure 11 Effect of hard segment length on E' and E'' . E'' has been multiplied by 0.1 for clarity.

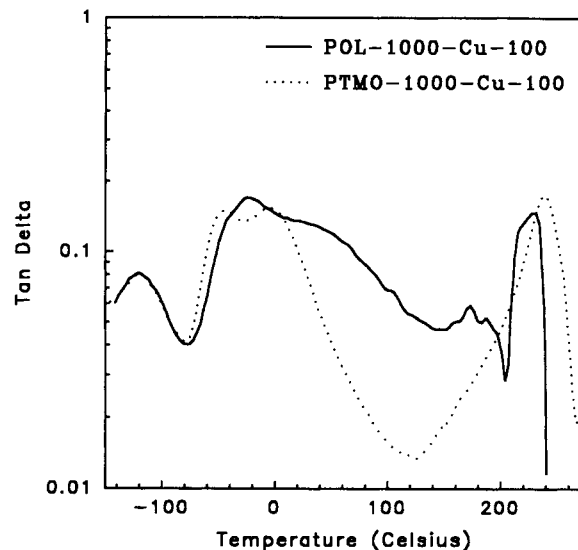


Figure 12 Effect of hard segment length on $\tan \delta$.

was 1000. If the phase purity of the soft segment were higher in PTMO-1000-Cu-100, then the glass transition would be lower. However, one would also expect the rubbery plateau modulus to be higher because the number of ionic groups in aggregates would be greater. The modulus of the PTMO diol-based material is only slightly greater than that of the POL-based material, and only at temperatures greater than 60°C. The lower glass transition of the PTMO diol-based materials is convincingly explained by an immobilization effect. Since the POL materials have three aromatic rings, one would expect the soft segment to be more tightly anchored, which would cause an increase in the soft segment glass transition relative to the PTMO materials.

IV. DISCUSSION

The $\tan \delta$ curves of these materials exhibited a maximum of four features: The transition at ca. -120°C is associated with localized motion of the methylene sequences of polyether segments.²⁷ The upper transition at ca. 250°C is associated with the ionic transition. The PTMO-1000-Cu-100 showed two additional transitions, as shown in Figure 12. The first corresponds to a soft-segment rich phase glass transition (ca. -40°C), whereas the second may correspond to a hard-segment phase transition (ca. 20°C).

All other curves had a very broad transition in the region between 0 and 100°C . In some cases, the transitions were very asymmetric, which might indicate two transitions. As can be seen in Figure 8,

asymmetry of this peak increases as the molecular weight increases, which supports the two transition hypothesis. The transition between 0 and 100°C is much narrower for the diol oligomer, which suggests that the hard segment is an important component of this broad transition.

Polyurethane ionomers based on TDI with no chain extender (one aromatic ring per hard segment) show a much more narrow and easily identifiable soft-segment glass transition at about -40°C, with no evidence of a broad transition in the region 0–100°C.^{2–4} PTMO–MDI-based polyurethane ionomers without a chain extender (two aromatic rings per hard segment) showed a small loss peak in modulus between 50 and 100°C, which the authors were unable to explain.^{10,11} Small-angle X-ray scattering (SAXS) studies found no indication of a three-phase morphology in the polyurethane ionomers without a chain extender, even in the materials with the small loss peak between 50 and 100°C.

The effect of chain extension on polyurethane ionomers was studied by Yang et al.¹² The hard segment in this case was MDI chain-extended with bis(hydroxymethyl)propanoic acid, which also contained the carboxylate functionality. The stoichiometry was adjusted to include an average of two MDI units per hard segment (four aromatic rings per hard segment) and also three MDI units per hard segment. The soft-segment glass transitions were much broader in these materials; however, no samples showed two peaks in DMTA spectra as was seen in PTMO-1000-Cu-100. SAXS curves exhibited a strong peak at $q = 0.5 \text{ nm}^{-1}$ and a very diffuse peak at $q = 3 \text{ nm}^{-1}$. The first peak was attributed to a hard-phase/soft-phase contrast, whereas the second was attributed to an ionic phase/polymer matrix contrast. The authors concluded that this system was separated into three phases. In two-phase systems, SAXS peaks due to an ionic phase/polymer matrix electron density contrast are usually significantly more intense and occur between $q = 1\text{--}2 \text{ nm}^{-1}$, which differs slightly from the observations of the three-phase system discussed above.

As discussed in the Introduction, the effect of ionization on already phase-separated polyurethanes has been studied. This work was based on polyurethanes made from PTMO–TDI prepolymers chain-extended with butanediol.¹³ Upon ionization, the upper temperature loss peak was observed at a relatively low temperature of ca. 150°C and the loss peak corresponding to the hard-segment glass transition at ca. 100°C disappeared. This result may indicate phase mixing of the aromatic rings and the ionic segments because the transition is intermediate between the glass transition of the two phases.

In chain-extended polyurethane ionomers, a three-phase morphology might be possible, although the factors governing such behavior are not well understood. The existence of a hard-segment-rich phase in amic acid ionomers can only be assessed by SAXS. Energetics should favor a separate three-phase system in amic acid ionomers as compared to polyurethanes because no chain extender is required to reach three aromatic rings per hard segment. DMTA studies of these materials indicate the possibility of three phases, but the evidence is not conclusive.

V. CONCLUSIONS

Novel ionomers have been synthesized from polyether polyamic acid segmented copolymers. These ionomers behave as thermoplastic elastomers, showing toughness and relatively high extensibilities. Similar to other ionomer systems, the ionic groups phase-separate into ionic domains. Cation type and degree of neutralization will affect phase separation, which, in turn, influences physical properties. The zinc-neutralized material showed less phase separation and markedly inferior tensile properties compared to the other ionomers. Decreasing soft-segment molecular weight led to an increase in modulus, more dramatic than aggregate density effects alone would predict. Aggregation into ionic-rich domains may cause an increase in chain entanglements, which act as effective cross-links in these ionomers. A filler effect of immobilized polymer matrix material could also explain the increase in modulus.

The number of aromatic rings per hard segment was altered as well. Distinct soft-segment and hard-segment transitions were present in the DMTA spectra with only one aromatic ring. DMTA spectra of materials with three aromatic rings showed very broad transitions from the region ca. -50 to 100°C. A three-phase morphology consisting of a soft-segment-rich phase, hard-segment-rich phase, and ionic-rich phase was discussed, but further work involving SAXS profiles will be required to confirm such a hypothesis.

This work was supported by a grant from the Department of Energy DE-FG02-88ER45370 and by a grant from the Petroleum Research Fund administered by the American Chemical Society 20343-AC7. B. P. G. would like to thank the Department of Defense for their support through a National Science and Defense Engineering Graduate Fellowship.

REFERENCES

1. See, e.g., A. Eisenberg and M. King, *Ion Containing Polymers*, Halsted-Wiley, New York, 1975.
2. Y. S. Ding, R. A. Register, C. Z. Yang, and S. L. Cooper, *Polymer*, **30**, 1204 (1989).
3. S. A. Visser and S. L. Cooper, *Macromolecules*, **24**, 2576 (1991).
4. S. A. Visser and S. L. Cooper, *Polymer*, **33**, 920 (1992).
5. Y. S. Ding, R. A. Register, C. Z. Yang, and S. L. Cooper, *Polymer*, **30**, 1213 (1989).
6. S. A. Visser and S. L. Cooper, *Macromolecules*, **24**, 2584 (1991).
7. Y. S. Ding, R. A. Register, C. Z. Yang, and S. L. Cooper, *Polymer*, **30**, 1221 (1989).
8. S. A. Visser and S. L. Cooper, *Polymer*, to appear.
9. D. C. Lee, R. A. Register, C. Z. Yang, and S. L. Cooper, *Macromolecules*, **21**, 998 (1988).
10. D. C. Lee, R. A. Register, C. Z. Yang, and S. L. Cooper, *Macromolecules*, **21**, 1005 (1988).
11. K. K. S. Hwang, T. A. Speckhard, and S. L. Cooper, *J. Macromol. Sci.-Phys.*, **B23**(2), 153 (1984).
12. C. Z. Yang, T. G. Grasel, J. L. Bell, R. A. Register, and S. L. Cooper, *J. Polym. Sci. Part B Polym. Phys.*, **29**, 581 (1991).
13. J. A. Miller, K. K. S. Hwang, and S. L. Cooper, *J. Macromol. Sci.-Phys.*, **B22**(2), 321 (1983).
14. D. P. Heberer, S. Z. D. Cheng, J. S. Barley, S. H.-S. Lien, R. G. Bryant, and F. W. Harris, *Macromolecules*, **24**, 1890 (1991).
15. C. E. Arnold, J. D. Summers, Y. P. Chen, R. H. Bott, D. Chen, and J. E. McGrath, *Polymer*, **30**, 986 (1989).
16. B. Masiulonis, J. Hrouz, J. Baldrain, M. Ilavsky, and K. Dusek, *J. Appl. Polym. Sci.*, **34**, 1941 (1987).
17. P. M. Hergenrother and S. J. Havens, NASA Case No. LAR-14-001-1, Pat. Appl. (November 9, 1989).
18. X. Yu, C. Song, C. Li, and S. L. Cooper, *J. Appl. Polym. Sci.*, **44**, 409 (1992).
19. B. Hird and A. Eisenberg, *J. Polym. Sci. Part B Polym. Phys.*, **28**, 1665 (1990).
20. W. W. Graessley, *Macromolecules*, **8**, 865 (1975).
21. P. J. Flory, *Proc. R. Soc. Lond. A.*, **351**, 351 (1976).
22. R. A. Register and S. L. Cooper, *Macromolecules*, **23**, 310 (1990).
23. C. E. Williams, T. P. Russell, R. Jérôme, and J. Horrion, *Macromolecules*, **19**, 2877 (1986).
24. J. J. Aklonis and W. J. Macknight, *Introduction to Polymer Viscoelasticity*, Wiley-Interscience, New York, 1983.
25. A. Eisenberg, B. Hird, and R. B. Moore, *Macromolecules*, **23**, 4098 (1990).
26. M. A. Vallance, J. L. Castles, and S. L. Cooper, *Polymer*, **25**, 1734 (1984).
27. A. Lilaonitkul and S. L. Cooper, *Advances in Urethane Science and Technology*, K. C. Frisch and S. L. Reegen, Eds., Technomic, Westport, CT, 1979, Vol. 7, p. 163.

Received January 9, 1992

Accepted February 27, 1992